

Real-time tsunami inundation forecast system using S-net data

AOI, Shin^{1*} ; YAMAMOTO, Naotaka¹ ; SUZUKI, Wataru¹ ; NAKAMURA, Hiromitsu¹ ; KUNUGI, Takashi¹ ; KUBO, Tomohiro¹ ; HIRATA, Kenji¹ ; MAEDA, Takahiro¹

¹NIED

One of the causes of escalation of damages during the 2011 megathrust Tohoku earthquake (M 9.0) was the underestimations of initial estimation for tsunami height of JMA forecast as well as the insufficient dissemination of the tsunami information to people due to power failures. To reduce the fatalities due to tsunamis, it is essentially important to deliver prompt and accurate forecast to the on-shore residences when a large tsunami is generated by a huge earthquake. At the time of the Tohoku earthquake, in the Pacific coasts of Kanto, Tohoku and Hokkaido districts, off-shore observations were insufficient and the observed data essential for efficient tsunami forecast was very poor. In response to this situation, Japanese government decided to construct S-net (Seafloor Observation Network for Earthquakes and Tsunamis along the Japan Trench; Kanazawa et al., 2012, JpGU; Uehira et al., 2014, AOGS; Uehira et al., 2015, JpGU) and NIED is now constructing this observation network under the sponsorship of MEXT, Japanese government. S-net consists of 150 ocean bottom observatories linked by ocean bottom fiber optic cables with the total length of approximately 5,700 km. This dense network covers the wide area of the Japan Trench and the southernmost Kuril Trench from Kanto to Hokkaido, and every source area of an earthquake of magnitude larger than 7.5 includes at least one observatory. One of the most important contributions of S-net is that we obtain additional lead time for earthquake and tsunami early warning. For the best case, the additional lead time by using data from S-net is about 20 minutes for a direct direction of a tsunami generated by an earthquake that occurs in the Japan Trench, and 30 seconds for earthquake early warning. To maximize the advantage of S-net, we are developing a new methodology of real-time tsunami inundation forecast system. Many tsunami forecast methods have been studied. For instance, Tsushima et al. (2012) proposed tFISH which estimates tsunami height by forward simulation using inverted source model and Baba et al. (2014) proposed a method using relationship of tsunami height between offshore and near coast. We select an approach to prepare tsunami scenario bank in advance for at least thousands of source scenarios and, when a tsunami occurs, a forecast is carried out by comparing observed ocean bottom pressure data and pre-calculated data, and selecting several possible scenarios to represent forecast uncertainties which can almost evenly explain observations according to a particular criteria (Yamamoto et al., 2014, AGU; Suzuki et al., 2015, JpGU), because inundation is a highly non-linear phenomenon and its calculation costs are rather heavy. An advantage of our method is that tsunami inundations are estimated explicitly without any source information which may have large estimation error, especially for real-time analysis. As the number of the tsunami scenarios stored in the bank is limited, due to heavy calculation loads for inundation simulations, for accurate forecast, it is important to appropriately assume the input source models. Therefore, we first carry out many calculations based on linear long-wave theory which only requires much less calculations comparing with nonlinear theory to check the sensitivities of the source models to coastal tsunami heights. Based on a large number of sensitivities analyses, we will construct the tsunami scenario bank that efficiently covers possible tsunami scenarios affecting the target region.

Keywords: tsunami, real-time tsunami forecast, tsunami inundation forecast, S-net

Examination of algorithms toward real-time tsunami forecast using ocean bottom pressure data

SUZUKI, Wataru^{1*} ; YAMAMOTO, Naotaka¹ ; AOI, Shin¹ ; HIRATA, Kenji¹ ; NAKAMURA, Hiromitsu¹ ; KUNUGI, Takashi¹

¹NIED

We are developing a method toward a real-time forecast of the tsunami inundation as well as the coastal tsunami heights using the real-time data observed by the Seafloor Observation Network for Earthquakes and Tsunamis along the Japan Trench (S-net; Uehira et al., 2015) and are constructing a prototype system that implements the real-time forecast method for the Pacific coast of Chiba prefecture (Sotobo region) (Aoi et al., 2015). In this study, we examine an algorithm for the real-time forecast using the data from the ocean bottom pressure gauges of the S-net. We employ the database-based method to forecast the inundation, which is a nonlinear phenomenon, for relatively broad region. We use the densely observed data set probably including the data obtained in or close to the tsunami source area to perform the rapid and precise tsunami forecast. The database is called as "Tsunami Scenario Bank" in this study and includes "Tsunami Scenario" composed of the possible tsunami source model, and the simulation results of the ocean bottom pressure data at S-net observation stations, coastal tsunami heights, inundation areas, and flow depth if inundation will occur, for each of the source models. Triggered by an earthquake or tsunami, the algorithm starts to search scenarios whose ocean bottom pressure data match the observed data reasonably well. Selected scenarios from this matching then provide the information of forecasted tsunami heights, inundation areas and flow depth, adequately considering the uncertainties of the forecast. Ideally, uncertainty of the forecast information becomes small as the tsunami generation and propagation are well captured by widely deployed seafloor observation network.

One of our examined algorithms selects scenarios by evaluating the match of the spatial distributions as snapshots between the observed and scenario offshore pressure data using multiple indexes (Yamamoto et al., 2014). The indexes for evaluation are the correlation coefficient of the observed and scenario pressure amplitudes, geometrical mean and geometrical standard deviation of the ratio of the observed to scenario data. Use of multiple indexes provides more robust scenario selection or tsunami forecast than use of single index. We also examine the two variance reductions whose L2-norm part is normalized either by the observed data or by the scenario data. The variance reduction with the normalization by the observed data is sensitive to the overestimation of the forecasted tsunami while that by the scenario data is sensitive to the underestimation. Use of both variance reductions together has a potential to more robustly constrain the size of the generated tsunamis. In addition to the above algorithm that evaluates the spatial snapshots of the tsunami propagation, we will further examine another approach that uses the time history of the tsunami waveform itself.

Keywords: Real-time tsunami forecast, Tsunami inundation, Scenario bank, S-net

A tsunami propagation modeling based on the adaptive mesh refinement

MAEDA, Takahiro^{1*} ; AOI, Shin¹ ; IWAKI, Asako¹ ; HAYAKAWA, Toshihiko²

¹NIED, ²Mitsubishi Space Software Co.,ltd.

For the efficient tsunami modeling, reduction of grid number is effective. It is important to construct the most suitable grid spacing according to the topography of the seabed and to connect the grids appropriately because the grid spacing depends on a propagation speed of tsunamis. A nesting is usually employed as the method to connect the grids and is suitable for the tsunami modeling for specific area. However, it is necessary to calculate several times to cover up a wider area in case of large tsunamis like the 2011 Tohoku tsunami. In this study, we employ the adaptive mesh refinement (AMR) by discretizing a domain spatially using tree-structure grid automatically based on the CFL condition.

Keywords: tsunami, simulation, adaptive mesh refinement, tree-structure grid

Retrospective evaluation of tFISH performance: Forecasting of tsunami caused by the M 7.3 earthquake on Mar. 9, 2011

HORIUCHI, Akiko^{1*} ; HINO, Ryota² ; OHTA, Yusaku¹ ; KUBOTA, Tatsuya¹ ; TSUSHIMA, Hiroaki³

¹Graduate School of Science, Tohoku University, ²International Research Institute of Disaster Science, ³Meteorological Research Institute, Japan Meteorological Agency

On March 9, 2011, the largest foreshock (Mw7.3) of the 2011 Tohoku-Oki earthquake occurred accompanying tsunami with amplitude of about 50 cm at coastal tide-gauge stations in Iwate and Miyagi prefecture. When the earthquake occurred, nine ocean bottom pressure gauges (OBPGs) were installed by Tohoku University around the epicenter, which recorded tsunami with amplitude of 10-30 cm. Kubota (2012) estimated the slip distribution of this earthquake from detailed analysis of the tsunami waveforms. These waveforms were obtained from retrieved OBPGs after the earthquake, however, these offshore data would contribute to an improvement of the accuracy of tsunami forecast if they were available in real-time.

We applied tFISH algorithm to this offshore tsunami data and calculated the waveforms of the coastal tide-gauge stations. We inverted the waveform data recorded offshore to estimate the distribution of the initial sea-surface height, synthesized tsunami waveforms at coastal tide gauge stations, and then compared the calculated waveforms with observations to evaluate the accuracy of the forecast. As a result, it turned out that coastal tsunami waveforms calculated 6 min after the earthquake, or 25 min before the arrival of the first wave to the coast show good agreements with observations in arrival times with misfits less than 2 min. Amplitudes were estimated in the range of 50 to 200 % of the tide-gauge records. This early and accurate forecast by the tFISH was achieved by dense coverage of OBPGs in the range of the tsunami source. The main packet of the tsunami signal reached the offshore stations within 6 min after the earthquake, making the initial sea surface height estimation accurate.

The results of this study demonstrate that tFISH can provide accurate forecast of tsunamis generated by frequent M7 class earthquakes when dense offshore observation networks are available in real-time.

Keywords: Near-field tsunami forecasting, ocean-bottom pressure gauge, tsunami waveform inversion

Investigation on Tsunami Source Inversion Methods for Real-time Inundation Predictions (2)

OISHI, Yusuke^{1*} ; IMAMURA, Fumihiko² ; SUGAWARA, Daisuke² ; FURUMURA, Takashi³

¹Fujitsu Laboratories LTD., ²International Research Institute for Disaster Science, Tohoku University, ³Earthquake Research Institute, the University of Tokyo

1. Background

In preparation for giant tsunamis, online observation networks of offshore tsunami and onshore ground deformation have been actively deployed. For instance, NIED is developing the S-net system that will consist of 150 observation stations and will cover wide areas around the Japan Trench. Some analysis methods that utilize the online observation networks and predict tsunami inundation in real time have been proposed so far. Most of them find the best-matched solution from the database of pre-computed inundation simulation results (e.g., Baba et al., 2012; Gusman et al., 2014; Yamamoto et al., 2014). Although the database approaches have an advantage of rapid analysis speed, it would be difficult to comprehensively deal with all the inundation situations caused by megathrust earthquakes of which fault rupture processes are complicated and spread across wide areas.

Another approach to predict the tsunami inundation after earthquakes occur is based on the real-time inundation simulation with the input of instantly predicted tsunami sources. The recent development of high-performance computing makes the inundation simulation rapid enough, and in most cases the simulations can be completed before tsunamis arrive at the coastline (e.g., Oishi et al., 2015). However, in terms of the instant tsunami source analysis method, the existing methods (e.g., Tsushima et al., 2014; Ohta et al., 2011) are designed to predict the arrival time and maximum wave height at the coastline and do not necessarily consider the accuracy of site-specific inundation predictions.

2. Tsunami Source Inversion Method for Real-time Inundation Prediction

Therefore, we develop a suitable source analysis method for accurate tsunami inundation predictions. Oishi et al. (2014, SSJ Fall Meeting) proposed an inversion method that put a high priority on the reproducibility of the observed waveform in the offshore regions near the high-resolution inundation prediction area (i.e., the innermost area of the nested grid system in inundation simulations), which enables to provide good prediction accuracy of the incident wave at the high-resolution inundation prediction area. In addition, in this study, we propose a method that incorporates the crustal deformation prediction based on onshore GPS geodetic observation data, which is very accurate in the inshore and inland regions. Our method predicts the sea-surface and crustal deformations in the landward side of offshore tsunami observation stations using only the GPS geodetic observation data and predicts the sea-surface deformation in the open-ocean side of offshore tsunami observation stations using the tsunami data. We expect that the present method can improve the accuracy of the inundation predictions by accurately incorporating the land subsidence as well as the sea surface deformation in the area of tsunami propagation path between the offshore tsunami source and land.

3. Application to the 2011 Tohoku-Oki tsunami

The present source analysis method is applied to the 2011 Tohoku-Oki tsunami and the resulting source models are used in the 5-m-resolution inundation simulations of Sendai and Miyako cities. As a result, the observed waveforms at the coastal areas are well reproduced demonstrating that the present method can accurately predict the incident wave at the high-resolution inundation prediction areas. The source model is repeatedly updated using the observed data of a longer time period and provides the well-converged incident waveform when sufficient data are used. After the convergence, the predicted inundated regions show good agreement with the observation.

Keywords: Inundation simulations, real-time tsunami source prediction

Construction of tsunami prediction system using tsunami amplification

TAKAHASHI, Narumi^{1*} ; ISHIBASHI, Masanobu¹ ; NAKAMURA, Takeshi¹ ; BABA, Toshitaka² ;
KANEDA, Yoshiyuki³

¹Japan Agency for Marine-Earth Science and Technology, ²University of Tokushima, ³Nagoya University

In the Nankai Trough area, possibility of huge earthquake with over M9 is pointed out. Therefore, local governments along the area revised estimation of many types of damages and planed action for the disaster prevention. The coastal area near the rupture zone, however, receives heavy tsunami within a few minutes according to Cabinet office of Japanese government. To take actions against severe situation, Japan Agency for Marine-Earth Science and Technology (JAMSTEC) constructed a tsunami immediate prediction system using dense ocean floor network system for earthquakes and tsunamis (DONET) based on concept of tsunami amplification.

Tsunami height strongly depends on the topography during tsunami preparation because the tsunami speed is expressed by a function of water bottom. Therefore, JAMSTEC had investigated the possibility for use of tsunami amplification for the tsunami prediction (Baba et al., 2013). With assurance of fault models, we calculated theoretical tsunami waveform for twenty DONET stations and targets of the coastal cities and got each maximum tsunami height. We selected Kushimoto town, Owase city, and Omaezaki city as first step of the system construction and constructed tsunami database including their tsunami waveforms and inundation maps. This system detects first arrivals of earthquake and tsunami using real-time DONET data, calculated average of absolute observed pressure values for twenty DONET stations, constructed a correlation profile between the average values and maximum tsunami height of each city, and select fault models changing the average values from the correlation profile. We introduce theoretical pressure waveform of the 1944 Tonankai earthquake and have considered method to make reduce the error of predicted tsunami height by this system. As a result, we found that it is important to select stations used for this system and fault models based on directions of detected events. In this presentation, we report concept of the tsunami immediate prediction system and future plan of the revise.

Keywords: tsunami amplification, immediate prediction, DONET, Nankai Trough

A new technique for tsunami numerical simulation using tsunami observations in a source region as an input

TANIOKA, Yuichiro^{1*}

¹Hokkaido University

After the 2011 devastating Tohoku-oki tsunami, improvement of tsunami warning system is one of key issues in Japan. Japanese government is decided to install 125 ocean bottom pressure sensors and seismometers with a cable system along the Japan and Kurile trench. More than 50 sensors have already been installed off Boso to Sanriku. The rest of them will be installed by March, 2016. We should take an advantage using those data for real-time tsunami forecast.

Although the tsunami is generated by coseismic deformation due to a large earthquake, sensors on the top of tsunami source area do not observe a large vertical coseismic deformation. They observe a tsunami wave when it starts to propagate. It will be a network of pressure sensors on the top of tsunami source area in near future. In this paper, a new technique, which uses the observations at a network of pressure sensors on the tsunami source area as an input to compute the tsunami, is presented.

In this technique, a time derivative of observed heights at sensors are used as an input to compute the tsunami. Actual tsunami heights at the sensors on the source area is difficult to know immediately because the coseismic vertical deformation is unknown. However, we observe directly the time derivative of tsunami heights at the sensors.

Equations of finite difference schemes using linear long wave equations with a staggered grid system are transformed. So, at first, time derivatives of tsunami heights at each grid are used as inputs. Then we can numerically compute a tsunami using a traditional finite difference technique. First, the technique was tested using the synthetic tsunami waveforms computed using 5 minutes grid system off Tohoku. Time derivatives of tsunami heights in 36 X 36 grids are used as an input to compute tsunami instead of coseismic deformation or ocean surface deformation. The tsunami computed from this new technique is consistent with the tsunami computed from the previous tsunami numerical simulation using the vertical ocean surface deformation as an initial condition. This result indicates that tsunami forecast using this technique do not need any information about the source of the earthquake but the observed tsunami waveforms near the source area.

Keywords: Tsunami numerical simulation, Tsunami forecast, S-Net, tsunami ocean bottom cable

A multi-grid algorithm for transpacific and regional tsunami modeling

HAYASHI, Kensaku¹ ; VAZHENIN, Alexander^{1*} ; MARCHUK, Andrey²

¹University of Aizu, Japan, ²ICMMG SB RAS, Russia

The material presented in this paper can be divided into two parts. The first is the implementation of algorithms for generating tsunamis in the course of numerical experiments as a result of the initial ellipsoidal water surface displacement or by boundary conditions. In the second part, the realization is described of *the multi-grid algorithm for tsunami computations*.

Tsunami sources are usually located in deep-water areas. So, if we want to estimate tsunami parameters near the coastline the computational domain must include both deep and shallow-water areas. A standard stability condition for numerical algorithms used for modeling requires the wave advancement at one time step be less than a spatial grid-step. In this case, we should use a small enough time step (for the computation stability in deep-water areas of the domain), which makes computations on a shallow shelf with an unreasonably small time step be too long.

The multi-grid algorithm for the tsunami propagation computations from the initial source to the coastline that uses scale switching has been developed. Computations are carried out on a sequence of grids with various resolutions where one is embedded into another. Tsunami wave parameters are transferred from the larger domain to the embedded smaller one by means of the boundary conditions. Using the method proposed the numerical modeling of tsunami generated by a model ellipsoidal source located in the middle of the Pacific was carried out. We are demonstrating that the proposed method effectively works in case of poor correlated gridded bathymetries with different resolutions as well as in using the pipeline computational scheme.

Keywords: Tsunami Numerical Modeling, Shallow-Water Model, Computational Grid, Grid Step, Boundary Conditions, Pipelined Computing

Tsunami-tide simulation: Early arrival time of tsunami due to tidal currents

NAKADA, Satoshi^{1*} ; HAYASHI, Mitsuru¹ ; KOBAYASHI, Ei-ichi¹ ; KOSHIMURA, Shunichi²

¹Graduate School of Maritime Sciences, Kobe University, ²International Research Institute of Disaster Science, Tohoku University

This study investigated influences of tides on a giant tsunami generated by the anticipated greatest scenario earthquake along the Nankai Trough by conducting tide-tsunami simulation in Osaka Bay as a pilot shallow ocean. It has been reported that Nankai Trough Earthquake will occur about 70 % of probability within 30 years in the future and drive the giant tsunami. The speed of the tsunami plus the tidal currents may exceed 2 knot (approximately 1 m/s) at many ports in the Japanese coasts facing to Pacific, in particular Seto Inland Sea. This speed can make difficult to operate the marine vehicles ships and escape from the port that the tsunami attacks according to the evacuation scenarios for ships and tsunami hazard maps. However, many tsunami simulations have hardly considered the factor of the tidal current. We conducted the tsunami simulation under the consideration of tidal current (i.e. tsunami-tide simulation) during three days from the earthquake occurrence. Our study area is Osaka Bay retaining many landfills in the nearshore area as a pilot ocean for the tsunami simulation. The high-resolution simulation with a horizontal resolution of 50 m was achieved by employing the nesting method to represent the complex coastal lines around the landfills along the bay coast. Our simulation showed that the tsunami intruding to the bay accelerates (decelerates) in the flood (ebb). As a result, the arrival time of tsunami to the coastline can be earlier (later) in the flood (ebb) than the tsunami without the tide. This indicated that the speed of tsunami intruding to the bay is enhanced (declined) by the advection of the flood (ebb) tide. We have revealed the relationship between the tidal phases and strengths of tsunami-tide interaction, demonstrating that the interaction can be significant in the strong flood and ebb tide due to the advection effect as the tidal waves enters to the coastal, shallow water regions. Further, our simulation showed that the tide-tsunami interaction was locally enhanced in the coastal oceans in front of the landfills in the eastern Osaka Bay. Thus, the tide-tsunami interaction is essential process to improve the model accuracy in the shallow coastal ocean and estimate the accurate arrival time of tsunami wave to coasts. Our results encourage that the realistic simulation of tsunami occurred in each tidal phase should be conducted to improve more safe evacuation scenarios or manuals prepared by effective and accurate hazard maps based on the time-tsunami simulation.

Keywords: Tsunami, Simulation, Tide, Marine Hazard, Nankai Trough Earthquake

Tsunami simulation with linear Boussinesq equations including elastic loading and seawater density stratification

BABA, Toshitaka^{1*} ; ALLEGER, Sebastien² ; CUMMINS, Phil² ; ANDO, Kazuto³ ; IMATO, Yoshiyuki³ ; KATO, Toshihiro⁴

¹Tokushima Univ., ²ANU, ³JAMSTEC, ⁴NEC

The tsunamis caused by the 2011 Tohoku and 2010 Maule earthquakes were clearly recorded at ocean-bottom pressure gauges distributed in the Pacific Ocean such as DART system. However there were significant discrepancies between the observed waveforms and those computed using standard shallow water theory. The observed waveform mainly took the form of a delay in the time of arrival and a small drawdown prior to the first-arriving positive peak in comparison with the computed waveforms. The discrepancies have been investigated by several papers (Tasai et al., 2013, Watada 2013, Inazu and Saito 2013, Alleger and Cummins 2014). To solve the discrepancies, they reached a conclusion to include effects of elastic deformation of the Earth loaded by tsunami and seawater density vertical stratification into the shallow water theory. On the other hand, frequency dispersion is often apparent in the far-field tsunami records, which can be simulated with the Boussinesq theory. Therefore, we included the effects of elastic loading and seawater density stratification into the Boussinesq equations to aim a comprehensive tsunami simulation. We embedded the module developed Alleger and Cummins (2014) into our Boussinesq tsunami code (Baba et al., 2015), and used it for the simulation of the 2011 Tohoku tsunami. The new model including dispersion effect provided a good agreement with the observations better than the without model at the far-field stations such as DART32401.

Keywords: Tsunami, Boussinesq, seawater density stratification, elastic loading

Early warning system of tsunami by measuring tsunamigenic ionospheric hole

KANAYA, Tatsuya^{1*} ; KAMOGAWA, Masashi¹

¹Dpt. of Phys., Tokyo Gakugei Univ.

Low frequency acoustic waves, termed infrasonic waves, are excited by the sudden displacement of ground and sea surface at large earthquake (EQ) and tsunami. When the acoustic waves propagate into the ionosphere, they disturb the ionospheric plasma. The plasma disturbance has been detected by the measurement of total electron contents (TEC) between a satellite of Global Positioning Systems (GPS) and its receivers on the ground. In addition to the acoustic waves, a TEC depression lasting for a few minutes to tens of minutes, termed tsunamigenic ionospheric hole (TIH), is formed by the large EQ with tsunami above the tsunami source area. The largest TEC depression appears 10 to 20 minutes after the main shock. In particular, it takes 20 minutes to identify the initial tsunami height for M9-class EQ only when we focus on the TEC depression to identify the height. In this paper, we propose alternative methodology to shorten 5 minutes to identify the initial tsunami height.

Keywords: Tsunami, Tsunamigenic ionospheric hole, Total electron content

3D numerical simulation of the tsunami-generated electromagnetic field using non-uniform thin-sheet approximation

KAWASHIMA, Issei^{1*} ; TOH, Hiroaki²

¹Graduate School of Science, Kyoto University, ²Earth and Planetary Sciences, Graduate School of Science, Kyoto University

A large ($M_w=8.1$) tsunamigenic earthquake occurred along the Kuril-Kamchatka trench on 13 January 2007. This event was of normal fault type (Ji, 2007; Yagi, 2007; Yamanaka, 2007; Lay et al., 2009) and was considered to be strongly associated with another tsunamigenic earthquake of thrust fault type that occurred on the landward slope of the trench on 15 November 2006. The 2007 fault geometry, however, was uncertain in the sense that the dipping direction (southeast or northwest) was not determined by previous reports so far (e.g., Yamanaka, 2007; Lay et al., 2009).

The 2007 tsunami propagated through the Pacific Ocean and was observed at many tide gauge stations, seafloor tsunami sensors and the Deep-ocean Assessment and Reporting of Tsunami (DART) system. Fujii and Satake (2008) estimated the slip distributions for this tsunami by waveform inversions and revealed insignificant difference between the two fault dips. Our seafloor electromagnetic (EM) station successfully observed tsunami-generated EM variations approximately one hour after arrival of seismic waves (Toh et al., 2011). The EM variations were generated by the coupling of the particle motion of conductive sea water with geomagnetic main field during tsunami passage. Some numerical simulations of the so-called motional induction process, viz., the tsunami dynamo effect, were conducted in two-dimensional (2-D) time domain (Minami and Toh, 2013) and three-dimensional (3-D) frequency domain (Zhang et al., 2014).

In this study, we introduced a 3-D non-uniform thin-sheet approximation proposed by McKirdy, Weaver and Dawson (1985). We newly developed a 3-D frequency domain code to calculate the tsunami dynamo effect, which was able to represent actual bathymetry by lateral conductance distribution within the surface thin-sheet without introducing many vertical grids in the ocean.

We applied this method to calculate the EM variations generated by tsunamis of the 2007 Kuril earthquake and estimated the slip distributions for both fault dips. As for kinetic tsunami propagation simulation, we used the linear Boussinesq approximation in order to reproduce subsequent phases after the tsunami first arrival. As for inversion, we used a non-negative least square method to fit the observed downward magnetic component as well as to avoid negative slips on the fault plane.

Our calculations indicate that the southeast-dipping fault model explains the observed downward magnetic component better than the northwest-dipping fault model. We also confirmed that the observed subsequent phases were produced by the frequency dispersion effect of the tsunami waves. The variance ratio (1.83) for the downward magnetic component by the two fault models was smaller than the critical F-value of 1.84 corresponding to 95% confidence level, although it passed the 90% confidence level. This may be attributed to too few observed data by the sparse sampling rate (2min). Use of more data such as the other tsunami-generated EM components can lead to determination of fault models with more accuracy. However, our calculation suggests that EM observations are sensitive enough to estimate the slip distribution on fault planes and can contribute to seismology.

Keywords: Tsunami, Dynamo effect

Three-dimensional simulation of the tsunami-generated magnetic fields: reproduction of seafloor tsunami magnetic signals

MINAMI, Takuto^{1*} ; TOH, Hiroaki¹ ; ICHIHARA, Hiroshi²

¹Graduate School of Science, Kyoto University, ²JAMSTEC

Electrically conductive seawater moving in the geomagnetic main field generates electric currents in the ocean. This is called "tsunami-generated electromagnetic (TGEM) phenomenon" and there have been many reports on electromagnetic (EM) data associated with this phenomenon since the occurrences of the recent extreme tsunami earthquakes, e.g., the 2011 Tohoku earthquake (e.g., Minami and Toh, 2013). TGEM phenomenon could be applied to the tsunami early warning, diagnoses of tsunamis, and inferences of the conductivity beneath the seafloor. However, each of these applications requires a highly accurate numerical simulation code that takes real bathymetry and arbitrary sub-seafloor conductivity structures into account and can reproduce the transient characteristics of TGEM fields.

For these applications, we developed a three-dimensional simulation code of TGEM fields, adopting the time-domain finite element method (FEM) with unstructured tetrahedral elements. Tetrahedral elements have an advantage in accurate expression of real bathymetry. In this simulation code, we first calculate the oceanic flow associated with tsunami propagation, solving the Laplace equation in terms of the velocity potential of the irrotational and incompressible seawater. Then, we conduct an electromagnetic (EM) simulation using the observed oceanic velocity field as a source. Use of the same tetrahedral mesh between hydrodynamic and EM simulations allows us to obtain the self-consistent results between them.

We conducted a TGEM simulation of the 2011 Tohoku earthquake tsunami with the tsunami source model presented by Satake et al. (2013). We compared the simulation results to the seafloor magnetic data observed on the eastern side of the Japan Trench and found that the amplitude of the calculated vertical magnetic component is less than the observed one, while they are nearly synchronized in phase. This result implies that the tsunami source model of Satake et al. (2013) could be improved by the tsunami magnetic field data.

In the presentation, we will report the comparison between the tsunami-generated magnetic data observed at the seafloor and the three-dimensional simulation results of the 2011 Tohoku earthquake tsunami. Furthermore, we will also report our attempt to infer a new tsunami source model that accounts for not only the existing sea surface elevation data but also TGEM field data.

Keywords: three dimensional simulation, finite element method, tsunami, magnetic field, tetrahedral elements, time domain

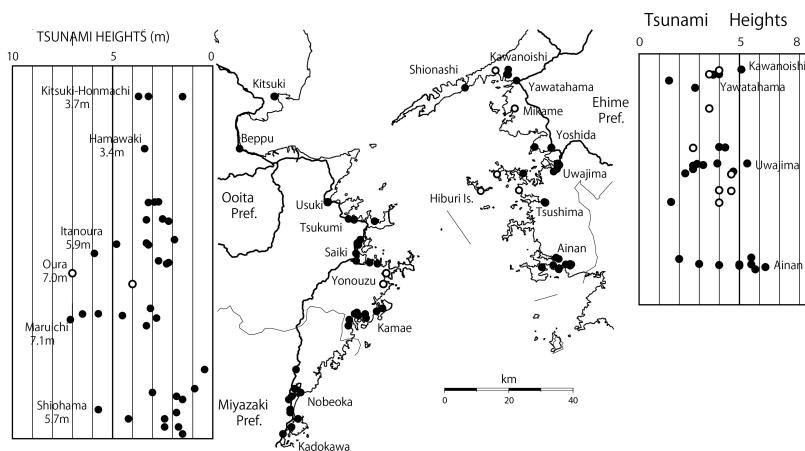
Tsunami Heights of the 1707 Hoei and the 1854 Ansei -Nankai earthquakes on the coasts of the Bungo straits

TSUJI, Yoshinobu^{1*} ; IWASE, Hiroyuki² ; MORIYA, Takumi² ; IMAI, Kentaro³ ; SATO, Masami³ ; HAGA, Yayoi³ ; IMAMURA, Fumihiko³

¹Fukada Geolog. Inst., ²Ecoh Co. Ltd., ³IRIDeS, Tohoku Univ.

We made field surveys of the height distributions of the tsunamis of the 1707 Hoei and the 1854 Ansei Nankai Earthquakes on the coasts of both side of Bungo straits, the coasts of Ehime Prefecture, Shikoku, and Ooita and Miyazaki prefectures, Kyushu by using a GPS level. On the coast of Ehime Prefecture, we made field survey the top of Sada cape to the southern boundary of the prefecture. Almost all of this area was the region of the clan of Date family, the lord of Uwajima Castle town. A detailed documents on damage of houses, rice field, and fishery vessels by the tsunamis were officially recorded. On Kyushu coast, Lord of Saeki castle recorded damage house and rice field damage of the 1854 Ansei tsunami for 21 coastal villages in the south part of Ooita Prefecture, Kyushu. The obtained height distribution of the tsunami of the 1854 Ansei Nankai earthquake is illustrated in the figure. Tsunami heights was 6.3 meters at Shimohisage village, Ainan town, Ehime prefecture, Shikoku, where all houses were swept away. Tsunami height of 7.1 meters was clarified at Takenoura and Maruichi villages, Ooita prefecture, Kyushu. The present study is financially supported by the Nuclear Regulation Authority.

Keywords: the 1854 Ansei Nankai Earthquake-Tsunami, the 1707 Hoei Earthquake-Tsunami, Bungo straits, Ehime prefecture, Ooita prefecture, Miyazaki prefecture



Maximum-level distributions of reflected waves from Chile and Hawaiian Islands in the 2011 Tohoku Tsunami.

ABE, Kuniaki^{1*} ; OKADA, Masami² ; HAYASHI, Yutaka²

¹none, ²MRI

Reflected waves of the 2011 Tohoku Tsunami were identified in the tide gauge records observed all over the Pacific Ocean and space distributions of the maximum levels were obtained. The digital records of 1 minute sampling for 64.3 hours from the origin time observed at 66 tide stations were used for analysis, which were summarized by ITIC. Main reflectors were assumed as ones from Chile and Hawaiian Islands. Reflected waves were separated from the time histories on arrival time of tsunami and duration time of large amplitude at the reflector or extension of the reflector. The maximum amplitudes were obtained and plotted as the geographical distributions. The result shows that the reflected waves were realized as an increase of sea level synchronizing to the arrival in a wide area. As for the reflected wave from Chile it is noticed that preceding propagation toward the pacific coast of central America and large-distance propagation arriving at Japan were observed (Fig.1). On the other hand reflected waves from Hawaiian Islands dominated in the same direction as a linear extension of Hawaiian Islands. It is noticed that maximum levels of the tsunami were attained by waves reflected from Hawaiian Islands at Kushimoto and Tosashimizu in Japan. Reflected waves except for the two were also observed. One of other dominant reflected wave is one from Californian coast, which was dominantly observed in north Pacific. .

Keywords: 2011Tohoku Tsunami, maximum level, reflected wave, Chile, Hawaiian Islands

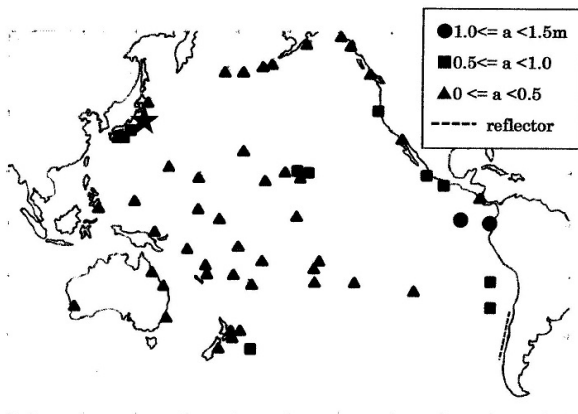


Fig. 1

Tsunami Heights and Period Distribution of Tokyo Bay and Characteristic Oscillation of Tokyo and Sagami Bays

TAKIGAWA, Akira¹ ; MUROTANI, Satoko¹ ; HEIDARZADEH, Mohammad¹ ; WU, Yifei¹ ; SATAKE, Kenji^{1*}

¹Earthquake Res Inst, Univ Tokyo

Coastal areas in Tokyo Bay have experienced earthquake tsunamis several times, and there is large difference in wave height distribution inside and outside the bay for tsunamis generated by near earthquakes (e.g. 1923 Kanto earthquake) and for those by far-field earthquakes (e.g. 2011 Tohoku earthquake). Significant attenuation of tsunamis results that wave heights at the inner part of Tokyo Bay were much smaller than those outside for the Kanto earthquake (Hatori et al., 1973), while less attenuation of the Tohoku earthquake tsunamis yielded similar tsunami heights inside and outside Tokyo Bay (Sasaki et al., 2012). Wave heights in a bay strongly depend on the period relation between incident wave and characteristic oscillation of the bay, so it is important to know about these. In this research, we conducted tsunami frequency analysis and calculation of characteristic oscillation for Tokyo Bay and surrounding area.

First, we conducted spectral analysis of observed and numerically reproduced waveforms and estimated the dominant periods. As a result, we found that dominant periods were different between two earthquakes, and that they were also different between inside Tokyo bay and outside Tokyo Bay (around Sagami Bay) even for the same earthquake. For example, the dominant periods were 70 and 30-40 min inside, and 110 min outside for the Kanto earthquake, while they were 60-70 min inside, 60-70 and 110 min outside for the Tohoku earthquake. These dominant period strongly affected wave heights in each area. In particular, for the Kanto earthquake, the shorter period (<40 min) component that was included in the first wave is responsible for the attenuation of tsunami heights around the mouth of Tokyo Bay, especially at the border connecting from Kurihama in Kanagawa Prefecture and Kanaya in Chiba Prefecture. The border is where the water depth becomes abruptly shallow when tsunamis enter the bay.

Second, we calculated characteristic oscillation of an area around Tokyo and Sagami Bays. Characteristic oscillations of Tokyo Bay have been calculated by Aida (1996) as solutions of the eigenvalue problem, but those of Sagami Bay have not. From tsunami numerical simulations, Imai et al. (2014) found the oscillation of Sagami Bay and its effects on tsunami behavior in Tokyo Bay. We consider wide areas including Tokyo and Sagami Bays, and solved an eigenvalue problem composed of linear shallow-water wave equation to obtain normal modes by the same method as Loomis (1975). As a result, we found that most modes were characterized by only inside Tokyo Bay (e.g. 112 min mode), but that several modes are characterized by outside or by both inside and outside (e.g. 72 min). Comparing these modes with dominant periods by frequency analysis, we found that dominant periods around 110 and 70 min periods could be explained by normal modes. However, 30 to 40 min periods that were detected outside for the Kanto earthquake could not be explained by normal modes, because there were no obtained modes correspond to them.

From above analyses and calculations, we consider the cause of the difference of attenuation. For the Kanto earthquake, shorter period (<40 min) components affected large wave amplitudes outside Tokyo Bay, but at the mouth of the bay they were weakened, and wave heights were accordingly attenuated from there. This could not be explained by characteristic oscillations, but Watanabe (1970) suggested that the wave reflection should have occurred and affected the attenuation, because of the abrupt decrease of water depth. On the other hand, for the Tohoku earthquake, the dominant period outside the bay was around 70 min that was close to the period of the coupled (inside and outside) mode of characteristic oscillation (72 min), so the oscillation could be transported to the inner part of the bay.

Keywords: Tsunami spectral analysis, Characteristic oscillation, Tokyo Bay, Sagami Bay, 1923 Kanto earthquake, 2011 Tohoku earthquake

Small-amplitude water oscillation near the coast generated by local crustal deformation of the 2011 Tohoku earthquake

KITO, Tadashi^{1*} ; NEMOTO, Makoto¹ ; OSADA, Masaki² ; HIRATA, Kenji²

¹OYO Corporation, ²National Research Institute for Earth Science and Disaster Prevention

Small-amplitude water oscillation is observed at several tsunami stations along the Pacific coast of the Tohoku region just after the origin time of the 2011 Tohoku earthquake and before arrivals of main tsunami waves. To investigate the cause of the small-amplitude water oscillation, we focus on the tsunami wave data recorded at the huge tsunami meters deployed by the Japan Meteorological Agency (JMA). We selected the data sets observed at the 3 stations (Miyako, Ofunato and Ayukawa) where the amplitude of the water oscillation is relatively high and waveforms are reasonably clear. The maximum amplitude of the water oscillation observed at the selected stations is about 50 cm, and the dominant period ranges from 60 s to 300 s.

Synthetic tsunami waveforms were calculated for the above-mentioned 3 stations using a tsunami simulation code in order to compare the observed waveforms of the water oscillation with the calculated ones. Firstly, uniformly distributed crustal displacement was assigned to all the mesh cells in the 50 m mesh-sized areas. The given crustal displacement changes in the time domain for 30 s based on the horizontal displacement of the GEONET data by Geospatial Information Authority of Japan (GSI) with the sampling rate of 1 s. The displacement data are obtained from the nearest GEONET station to each tsunami station (Miyako, Ofunato and Ayukawa). Second, tsunami simulation was carried out based on the non-linear shallow water theory using the created crustal deformation data and tsunami waveforms were calculated at the selected tsunami stations. Finally, a band-pass filter was applied to the calculated tsunami waveforms and the observed ones to alleviate the contamination of short-period noise and the long-period trend related to the main tsunami waves. Cross-correlation coefficients between the calculated tsunami waveforms and the observed ones were subsequently calculated to estimate the coherency of those waveforms.

A comparison of the calculated waveforms and the observed ones indicates that the observed small-amplitude water oscillation may be generated by the horizontal displacement near the Pacific coast in the Tohoku region due to faulting of the 2011 Tohoku earthquake. In addition to the similarity between calculated waveforms and observed ones, the dominant period of the observed water oscillation is consistent with the theoretically calculated natural period of water oscillation trapped in the bay. Since relatively small earthquakes along the plate boundary do not produce such large crustal deformation near the coast, this phenomenon may be characteristic of great earthquakes such as the 2011 Tohoku earthquake.

Tsunami source of the earthquake doublet on Dec. 7 2012 derived from near-field records by ocean bottom pressure gauges

KUBOTA, Tatsuya^{1*} ; HINO, Ryota² ; OHTA, Yusaku¹ ; SUZUKI, Syuichi¹ ; INAZU, Daisuke³

¹Graduate School of Science, Tohoku University, ²International Research Institute of Disaster Science, Tohoku University, ³UTokyo Ocean Alliance, The University of Tokyo

On December 7, 2012, an earthquake doublet occurred in the Pacific Plate near the Japan Trench. Both earthquakes had magnitudes of Mw 7.2 and the early one was estimated to have a reverse faulting mechanism with a focal depth of about 55 km, followed by a normal faulting earthquake occurred at a depth of about 20 km. The accuracy of the hypocenter locations based on the seismic waveform analysis is not high; some studies estimated that the second earthquake occurred at the landward of the Japan Trench (Global CMT; JMA) whereas Lay et al. (2013) and Harada et al. (2013) showed that it occurred at the seaward of the Japan Trench. 17 ocean bottom pressure gauges (OBPs) were deployed by Tohoku University near the epicentral area and high-quality waveform data of the tsunami associated with the doublet were recorded. The analyses of near-field tsunami waveform will improve the accuracy of the hypocenter location and help to understand the generation process of this unique intraplate doublet. We carried out forward calculations of tsunami waveforms based on the previously obtained CMT solutions. The observed tsunami was modeled best assuming the Global CMT solution, in which the second shallow earthquake is located beneath the landward slope of the Japan Trench. We also calculated tsunami assuming the tsunami source model derived from far-field tsunami records (Inazu and Saito, 2014). The calculated waveforms matched well to the observation in arrival times but calculated amplitudes were systematically smaller than the observations. We inverted the near-field tsunami waveforms for the initial sea-surface height distribution. The estimated pattern resembled well to the tsunami model by Inazu and Saito (2014) and that calculated from the Global CMT solution. However, the far-field tsunami waveforms calculated by our tsunami model did not fit the observations completely in their amplitudes. These results of our preliminary modelings suggest us that the horizontal locations of the tsunami sources estimated by these previous studies are consistent with near-field observations but there is still a room for improvements in depth and slip amount of the faults, reflecting the observed tsunami amplitude. As a future study, we will investigate the reliability of the static coseismic shift recorded by the OBPs near the epicenters and improve tsunami source model by including far-field tsunami waveforms.

Keywords: tsunami, doublet earthquake, tsunami source model, ocean bottom pressure gauge

Magnitude of the North Chile Earthquake Tsunami of April 1, 2014

HATORI, Tokutaro^{1*}

¹None

In seismic gap, a tsunami was generated off the coast of North Chile at 23:46(UTC)on April 1, 2014. The epicenter of the main shock was located at 19.642 S, 70.817W with a depth of 20.1 km and earthquake magnitude of M8.2 (USGS). The source area estimated by means of an inverse refraction diagram is 400 km length, extending N-S direction on the bathymetric line of 3,000 m. This location covers the source area of the 1877 tsunami. The tsunami began with up-direction at five tidal stations around the source area. It suggests that the sea-bottom of the source area uplifted. Judging from the attenuation of tsunami height with distance, tsunami magnitude to be $m=3$ that the grade is the mean value for earthquake magnitude. Magnitude of another tsunami accompanying with aftershock (M7.7) is $m=2$. Tsunami heights caused by the main shock are 200 cm at Arica and 184 cm at Iquique ,that values are normal for tsunami magnitude. According to tidal records (NOAA), about 60 cm at Hawaii , Fr. Polynesia and Iwate-Kuji are conspicuously large. The pattern of amplitude distribution is similar to other Chilean tsunamis.

Keywords: Tsunami source area, Tsunami magnitude, Distribution of tsunami heights

A set of characterized earthquake fault models for the probabilistic tsunami hazard assessment in the Nankai Trough

TOYAMA, Nobuhiko^{1*} ; HIRATA, Kenji¹ ; FUJIWARA, Hiroyuki¹ ; NAKAMURA, Hiromitsu¹ ; MORIKAWA, Nobuyuki¹ ; OSADA, Masaki¹ ; MATSUYAMA, Hisanori² ; KITO, Tadashi² ; MURASHIMA, Yoichi³ ; AKIYAMA, Shinichi⁴

¹NIED, ²OYO CORPORATION, ³KOKUSAI KOGYO CO., LTD., ⁴CTC (ITOCHU Techno-Solutions Corporation)

A set of characterized earthquake fault models are necessary for nation-wide probabilistic tsunami hazard assessment in Japan (Fujiwara et al., 2013; Hirata et al., 2014). It should include all possible earthquakes in future and should take into account various types of uncertainty. We introduced our strategy to construct a set of characterized earthquake fault models for tsunami hazard assessment in Japan, showing examples of earthquake fault models along the Japan Trench (Toyama et al., 2014).

In this study, we introduce a set of characterized earthquake fault models for tsunami hazard assessment in the Nankai Trough region, referring to the "Long-term Evaluation of earthquakes in the Nankai Trough region (2nd edition)" (2013/5/24) by the Headquarters for Earthquake Research Promotion (HERP), which was revised based on the lessons learned from the Great Tohoku earthquake.

At first, we classify tsunamigenic earthquakes into two categories as tsunami source fault specified or not.

And we classify specified tsunami source fault models as follows; 1) basic (typical) models, in which we put "large slip area (LSA)" under the characterization rule a) we will mention later, referring to the LSA configuration of the previous studies for the past large earthquakes occurred in the Nankai Trough region, 2) extended models, in which we put LSAs in various and possible configuration.

In addition to these models, we make "recurrence models", in which we put the source area corresponding to the historical tsunamigenic earthquakes and the simplified LSAs configuration based on the previous studies for the past large earthquakes. The total number of assumed earthquakes becomes 85, the 15 kinds of earthquakes shown in the "Long-term Evaluation" and possible 70 kinds of earthquakes.

Next, seismic moment, M_0 , to a characterized earthquake fault model, is determined by an empirical scaling relation between M_0 and fault area, S . We applied the relationship same as the one applied in the second phase report of the investigative commission for possible giant earthquake in the Nankai Trough region (2012) by Cabinet Office. There are some previous studies suggesting that rigidity is depth dependent, but we use a constant value of $5 \times 10^{10} (\text{N/m}^2)$ as rigidity.

We introduce inhomogeneity in earthquake fault slip to define LSA and "extremely large slip area (ELSA)" by the same rule applied in a set of characterized earthquake fault models along the Japan Trench as follows: a) LSA has twice slip amount as average slip and 30% area of the entire fault area (Korenaga et al., 2014). b) LSA is allowed to be located half pitch for along-trench direction and basically 3 patterns for trench-normal direction. c) ELSA can be allowed to be located along the upper edge in a LSA when the LSA is located adjoined the trench axis and has 4 times slip amount as average slip. d) The overlap rate for LSA is about a half to three fourths. e) The overlap rate for ELSA is about a half.

For unspecified earthquakes, we consider only a LSA at the center of the entire fault area. In this case, variability of possible LSA location is taken into account by introducing an uncertainty value of possible LSA location in process of tsunami hazard curve calculation (Fujiwara et al., 2013; Hirata et al., 2014).

A set of characterized earthquake fault models that we place in the Nankai Trough region, spans from M_w 7.7 to 9.2 for 85 kinds of earthquakes. Total number of the models in the Nankai Trough region reaches a little less than 4,000 in total. We are conducting non-linear tsunami simulations for all characterized earthquake fault models now.

This study was done as a part of the Management Expenses Grants project in NIED.

Keywords: tsunami hazard assessment, probability, characterized earthquake fault model, Nankai Trough

Tsunami simulation using seabed displacement due to fault slip obtained by boundary integration

AKIYAMA, Shinichi^{1*} ; FUJIWARA, Hiroyuki² ; HASHIMOTO, Norihiko¹ ; KORENAGA, Mariko¹ ; ABE, Yuta¹ ; MATSUYAMA, Hisanori³ ; MURASHIMA, Yoichi⁴

¹ITOCHU Techno-Solutions Corporation, ²National Research Institute for Earth Science and Disaster Prevention, ³OYO Corporation, ⁴KOKUSAI KOGYO CO., LTD

Initial water level of tsunami is generally considered equal to seabed displacement due to fault slip in simulation of tsunami which is generated by earthquake. Exact solution for displacement due to rectangular fault slip in elastic half space (Okada, 1985) has been widely applied to obtain the seabed displacement numerically.

On the other hand, we developed a new method to calculate the seabed displacement using boundary integration (Akiyama, et al. 2014). Our proposed method has advantages to calculate the seabed displacement easily only with the boundary integration for the fault surface, considering the seabed as an elastic half space and applying the Green's function which satisfies the free surface boundary condition, and to calculate the displacement adopting the irregular fault plane faithfully. The proposed method also has a feature that we can remove perfectly the influence of singularity of Green's function applying the Projection and Angular & Radial Transformation (PART) method (Hayami and Brebbia, 1988), when a fault plane is near from a seabed surface.

In this study, first, we calculate the seabed displacement due to the fault slip which is expected to occur in the plate boundary of the subduction area around Japan using the exact solution by Okada and the proposed method to compare the both results. Second, we execute tsunami simulations which the initial water level is considered equal to these displacements obtained above, and examine the difference between both results.

This research was carried out as part of Tsunami Hazard Assessment for Japan by National Research Institute for Earth Science and Disaster Prevention (NIED).

Reference

- Okada, Y. (1985) Surface deformation due to shear and tensile faults in a half-space, *Bull. Seism. Soc. Am.*, 75, 1435-1154.
Akiyama, S., H. Fujiwara and N. Hashimoto (2014) A new calculation method for seabed displacement due to fault slip by boundary integration, *JpGU 2014*, HDS27-14
Hayami, K. and C.A. Brebbia (1988) Quadrature methods for singular and nearly singular integrals in 3-D boundary element method, (Invited paper), *Proc. 10th Int. Conf. on Boundary Elements*, Southampton, Computational Mechanics Publication with Springer-Verlag, Vol. 1, pp. 237-264

Keywords: boundary integration, plate boundary, seabed displacement, tsunami simulation

Probabilistic tsunami inundation hazard assessment using detailed surface model

SAITO, Ryu^{1*} ; MURASHIMA, Yoichi¹ ; MURATA, Yasuhiro¹ ; INOUE, Takuya¹ ; TAKAYAMA, Jymnpei¹ ; AKIYAMA, Shinichi² ; MATSUYAMA, Hisanori³ ; HIRATA, Kenji⁴ ; FUJIWARA, Hiroyuki⁴

¹KOKUSAI KOGYO CO., LTD., ²CTC (ITOCHU Techno-Solutions Corporation), ³OYO Corporation, ⁴NIED (National Research Institute for Earth Science and Disaster Prevention)

A probabilistic tsunami inundation hazard for a city is described, as part of the probabilistic tsunami hazard assessment research work which has been promoted by NIED. Our study is primarily motivated by a need to understand that information of tsunami inundation hazard on a tsunami run-up area in a whole city contributes to the utility of disaster prevention plans and risk assessment.

The probabilistic tsunami hazard assessment for Japan has been conducted to estimate frequency of exceedance wave height along coastal regions [Hirata et al., 2014, JPGU], which is probabilistically derived from numerical modelling of tsunami sources as much consideration as possible. This tsunami run-up simulation has been implemented as a surface model at 50 m of minimum along coastal regions, however, which is not enough resolution to form an inhomogeneity of terrain topography and built structures, levees and seawalls, in finer resolution than 50 m. Then, a tsunami run-up simulation using higher spatial resolutions is important to quantify a tsunami inundation hazard for a city that includes several built structures and formation of inhomogeneous topography. With using the finer surface model above, different tsunami inundation hazards are quantified by a comparison between a potential inundation hazard without any structures and an inundation hazard protected with structures, which will be applicable for a performance of levees.

Here our study provides a technical note for quantification of probabilistic tsunami inundation hazard assessment for a city, Rikuzentakata one of example, using inundation information obtained from tsunami run-up simulation run at horizontal resolution 10 m with the many tsunami sources. A comparison between (1) a potential inundation hazard without any structures and (2) the other inundation hazard with structures is discussed. Earthquake scenarios used in this study are set by 1890 tsunami sources and occurrence frequencies around Japan trench [Touyama et al., 2014, JPGU], based on the long-term evaluation. The surface model of 10 m horizontal resolution is created from Airbone lider-derived high resolution surface model. This surface model contains built structures. The tsunami run-up simulation is carried out by a nested grid system consisting of five sub-regions from outer 2430 m to inner 10 m. The built structures are rigid, i.e. completely protect against tsunami overtopping and breaching levees, because of finding a simple interpretation of minimum inundation hazard compared to the potential inundation hazard, first of all. The probabilistic tsunami hazard assessment is quantified using much inundation information of area and depth in the city, resulted from the 1890 scenario's simulations.

We concluded that increasing model horizontal resolution clearly improved the tsunami inundation mapping and thus quantified the tsunami inundation hazard in detail. This ongoing study will lay a solid foundation for obtaining reliable tsunami inundation hazard in a city and for a cost-benefit analysis. Studies in probabilistic hazard analyses are also underway to implement uncertainty into tsunami inundation information [Abe et al. 2014, JPGU], which offers a more accurate estimates of the plausible inundation hazard.

Keywords: Tsunami, Inundation, Hazard assessment, Probability

Integration of hazard curves in Probabilistic Tsunami Hazard Assessment in Japan

ABE, Yuta^{1*} ; KORENAGA, Mariko¹ ; AKIYAMA, Shinichi¹ ; MATSUYAMA, Hisanori² ; MURASHIMA, Yoichi³ ; FUJIWARA, Hiroyuki⁴

¹ITOCHU Techno-Solutions Corporation, ²OYO Corporation, ³KOKUSAI KOGYO CO., LTD., ⁴National Research Institute for Earth Science and Disaster Prevention

Probabilistic Tsunami Hazard Assessment (PTHA) requires to simulate occurrences of several types of earthquake. We construct tsunami source models for each type of earthquakes and conduct numerical simulation of them to predict tsunami heights. Hazard curves for earthquakes are calculated by using predicted tsunami heights and setting occurrence probabilities, and then integrated to one hazard curve which assesses total tsunami hazard at a coastal site. We introduce a practical example of PTHA, specifically focus on the type of "off the Pacific coast of Tohoku Earthquake", and discuss a method for integration of tsunami hazard curve.

In order to take account for the uncertainties, we construct 106 tsunami source models for the type of off the Pacific coast of Tohoku Earthquake, which are difference in source region, magnitude, and slip distribution. As the first process of integration, we set weights for each source model. A tsunami height probability density distribution are calculated from tsunami heights and weights of each source model, and a hazard curve is calculated by multiplying the probability density distribution by the occurrence probability of off the Pacific coast of Tohoku Earthquake. The probability density distribution is depend on the setting rule of weight.

We experimentally examine PTHAs assuming different four weight setting rules. Mean values and standard deviations of the probability density distributions are calculated and compared to the observed tsunami heights in 2011 off the Pacific coast of Tohoku Earthquake. In one setting rule, which meet the policy of setting weights in the National Seismic Hazard Maps for Japan, mean $+1\sigma$ values are smaller than the the observed tsunami heights at almost every costal sites of Tohoku. By setting larger weights for the source models which have the magnitude of 9.1, or have large slip amounts near trench axis, mean $+1\sigma$ values become larger and include the observation values.

This study was conducted by a part of research project in NIED for tsunami hazard assessment for the whole of Japan.

Keywords: tsunami, hazard assessment, probability

Risk assessment of a tsunami caused by a large-scale sector collapse - Damage estimation of the Sakura-jima collapse -

YANAGISAWA, Hideaki^{1*}

¹Department of Regional Management, Faculty of Liberal Arts, Tohoku Gakuin University

A large-scale sector collapse due to volcanic activities sometimes flows into sea area and generates destructive tsunami disaster. In Japan, large-scale sector collapses and following tsunamis that killed more than several hundred people were occurred at least 3 times after the year 1603 (Edo era). The worst of them is the sector collapse of Mt. Mayuyama collapse in 1792. The following tsunami was widespread across Ariake sea and killed 15,000 people. Although a tsunami due to sector collapses is much less often than that of earthquakes, they can cause unexpected disaster. The aim of this study is to estimate tsunami risk by a large-scale sector collapse using GIS system and conduct detailed simulation of the sector collapse and following tsunami for a high-risk active volcano.

We first estimated the flow range of the sector collapse of active volcanos in Japan and overlaid them on sea area data using GIS to confirm whether the debris flows into sea area. Next, we searched populations around active volcanos to extract volcanos prone to cause human damage. Using these information and active level of volcano, we ranked tsunami risk of active volcanos. As a result, we found that Mt. Sakura-jima is the highest risk active volcano for tsunami disaster.

We further conducted the integrated simulation of landslide and tsunami. Here, we assume that volume of the sector collapse is same as 1640 Mt. Komagatake collapse. According to numerical results in the worst-case, approximately 1,000 people are buried by the debris of Mt. Sakura-jima collapse and following tsunami with 50 m heights attacks the coast of the Kagoshima city. The tsunami inundates 0.16 million home and 0.34 million people. These results indicated that large-scale sector collapse and following tsunami could cause one of the most destructive disasters and we need to consider a response for the worst disaster scenario.

Keywords: Tsunami, Sector collapse, Landslide, Simulation, Sakura-jima, Damage estimation